RSC Advances

PAPER

View Article Online
View Journal | View Issue

Open Access Article. Published on 13 November 2018. Downloaded on 1/16/2025 7:43:59 AM.
This article is licensed under a Creative Commons Attribution-NonCommercial 3.0 Unported Licence.

Check for updates

Cite this: *RSC Adv.*, 2018, **8**, 38013

A novel resource utilization method using wet magnesia flue gas desulfurization residue for simultaneous removal of ammonium nitrogen and heavy metal pollutants from vanadium containing industrial wastewater

Dean Fang,[ab] Xuefei Zhang[ab] and Xiangxin Xue*[ab]

In the present study, a novel resource utilization method using wet magnesia flue gas desulfurization (FGD) residue for the simultaneous removal of ammonium nitrogen (NH_4–N) and heavy metal pollutants from vanadium (V) industrial wastewater was proven to be viable and effective. In this process, the wet magnesia FGD residue could not only act as a reductant of hexavalent chromium [Cr(VI)] and pentavalent vanadium [V(V)], but also offered plenty of low cost magnesium ions to remove NH_4–N using struvite crystallization. The optimum experimental conditions for Cr(VI) and V(V) reduction are as follows: the reduction pH = 2.5, the wet magnesia FGD residue dose is 42.5 g L^{-1}, t = 15.0 min. The optimum experimental conditions for NH_4–N and heavy metal pollutants removal are as follows: the precipitate pH = 9.5, the $n(Mg^{2+}) : n(NH_4^+) : n(PO_4^{3-})$ = 0.3 : 1.0 : 1.0, t = 20.0 min. Finally the NH_4–N, V and Cr were separated from the vanadium containing industrial wastewater by forming the difficult to obtain, soluble coprecipitate containing struvite and heavy metal hydroxides. The residual pollutant concentrations in the wastewater were as follows: Cr(VI) was 0.047 mg L^{-1}, total Cr was 0.1 mg L^{-1}, V was 0.14 mg L^{-1}, NH_4–N was 176.2 mg L^{-1} (removal efficiency was about 94.5%) and phosphorus was 14.7 mg L^{-1}.

Received 21st September 2018
Accepted 26th October 2018

DOI: 10.1039/c8ra07876a

rsc.li/rsc-advances

Introduction

Sulfur dioxide (SO_2) is one of the primary atmospheric pollutants attributed to the burning of fossil fuels, and the emission of SO_2 leads to acid precipitation, vegetation destruction, and airborne particulate matter.[1,2] Out of all the emission sources of oxysulfide in China, thermal power plants are primarily responsible, and the flue gas desulfurization (FGD) system is the main method used for reducing SO_2 because it is a mature method and is widely used by the majority of the thermal power plants.[1–4] The FGD technologies can be roughly divided into three methods: wet processes, semi-dry processes and dry processes. Of all these methods, the take-up rate of use of wet FGD processes was about 85% for worldwide use of FGD technology because of its high efficiency and wide applicability. In the past few decades, the wet limestone–gypsum process was the mainstream technology, which had a take-up rate of about 90% for the reduction of SO_2 emissions in China.[4–6] It is worth noting that the wet magnesia FGD technology has been gradually applied to thermal power plants in China. Compared with the conventional wet limestone–gypsum process, wet magnesia FGD technology has many merits, such as high and stable desulfurization efficiency, simple and compact flow sheet, low investment and energy consumption. In particular, China has the most abundant reserves of the magnesite mineral, which has encouraged the development of wet magnesia FGD technology.[7–9]

The mechanism of the wet magnesia FGD process is similar to the wet lime–gypsum method. In the wet magnesia FGD process, magnesium hydroxide slurry is used as the SO_2 absorbent, which is prepared using an aging treatment of a mixture of magnesium oxide and water at a particular ratio. After removing the dust, the flue gas entered the absorption tower, and the SO_2 in the flue gas was subsequently absorbed by small magnesium hydroxide droplets from the spraying system. Therefore, the SO_2 in the flue gas could be removed and fixed in the desulfurization slurry because of the formation of low solubility magnesium sulfite.[2,7–11] After the slurry has reached the saturation absorption, the desulfurization product can be separated from the spent slurry by filtration to form the FGD residue, and the main composition of the FGD residue is magnesium sulfite hydrate.

At present, the main resource utilization method of the wet magnesia FGD residue was recovery of magnesium sulfate using

[a]Department of Resource and Environment, Northeastern University, Shenyang, 110819, PR China. E-mail: 123767899@qq.com; xuexx@mail.neu.edu.cn
[b]Liaoning Key Laboratory of Recycling Science for Metallurgical Resources, Shenyang 110819, PR China

Open Access Article. Published on 13 November 2018. Downloaded on 1/16/2025 7:43:59 AM.
This article is licensed under a Creative Commons Attribution-NonCommercial 3.0 Unported Licence.

forced catalytic oxidation and crystallization. The current research focuses on the development of a low cost and highly efficient catalyst.[2,12–14] As well as the regeneration of activated magnesia for FGD and regeneration of SO_2 for acid making using thermal decomposition of wet magnesia, FGD residue was also an attractive approach. But the oxidation of the magnesium sulfite should be prevented by adding an oxidation inhibitor during the FGD process because of the higher thermal decomposition temperature of magnesium sulfate.[8,9,15,16] Nowadays, the vast majority of the wet magnesia FGD residue is casually stacked without further treatment or discarded after forced aeration oxidation, and this is attributed to the high investment associated with the equipment for the treatment process and the low economic benefit of recycled products.[7]

The wastewater discharged from the sodium roasting vanadium extraction technology is complex, hard to degrade biochemically, has a high pollutant gas concentration, and is a highly hazardous acidic wastewater containing high concentrations of vanadium (V), hexavalent chromium [Cr(VI)] and ammonium nitrogen (NH_4–N).[17–20] The pollution emission concentration ranges of Cr(VI), total chromium, vanadium and NH_4–N in the wastewater were approximately 2500–4500 mg L^{-1}, 3000–5000 mg L^{-1}, 30–150 mg L^{-1} and 2000–3500 mg L^{-1}, respectively. According to the national discharge standard of pollutants for the vanadium industry (GB 26452-2011), the residual concentration of Cr(VI), total Cr, V and NH_4–N in the wastewater must be below 0.5 mg L^{-1}, 1.5 mg L^{-1}, 1.0 mg L^{-1} and, 40 mg L^{-1}, respectively. In reality, the heavy metal pollutants of the vanadium containing industrial wastewater were treated using chemical reduction precipitation, where the NH_4–N was treated using air stripping or struvite precipitation. In the traditional treatment progress, a lot of reagents were consumed, such as the reductants for the heavy metal removal, and the magnesium salts for the NH_4–N removal.[5,7]

In this study, a novel resource utilization of the wet magnesia FGD residue for simultaneous removal of NH_4–N and heavy metal pollutants from the vanadium containing industrial wastewater is presented. In this process, the wet magnesia FGD residue could not only reduce the Cr(VI) and V to Cr(III) and V(IV) which were low in toxicity and easy to separate under neutral conditions, but also offered plenty of low cost magnesium ions for removing ammonium using struvite crystallization. Therefore, the wet magnesia FGD residue could simultaneously remove V, Cr and NH_4–N from wastewater by forming the difficult to obtain, soluble coprecipitate containing struvite and heavy metal hydroxides. Compared with the conventional methods, this technology not only reduced the treatment cost of vanadium containing industrial wastewater and wet magnesia FGD residue, but also achieved the excellent objective of "waste treated by waste".

Materials and methods

Wet magnesia flue gas desulfurization residue

The wet magnesia FGD residue used in this work was provided by the Datang Lubei thermal power plant in the Shandong province of China. Because the residue was stacked at a waste landfill site for about three months under natural conditions, the FGD residue could be crushed directly and stored in a plastic valve bag. The chemical composition of the wet magnesia FGD residue was as follows (wt%): magnesium oxide (MgO): 25.9, sulfite (SO_3^{2-}): 23.75, sulfate (SO_4^{2-}): 12.81, silicon dioxide (SiO_2): 3.35, calcium oxide (CaO): 1.56, chloride (Cl): 0.72, carbonate (CO_3^{2-}): 6.75, TFe: 0.23. The results of the X-ray diffraction (XRD) analysis of the wet magnesia FGD residue are shown in Fig. 1(a), and the peaks of the wet magnesia FGD residue were consistent with those of magnesium sulfate trihydrate ($MgSO_3 \cdot 3H_2O$, JCPDS no. 00-024-0738), magnesium carbonate ($MgCO_3$, JCPDS no. 00-008-0479), magnesium sulfate hexahydrate ($MgSO_4 \cdot 7H_2O$, JCPDS no. 00-036-0419), and magnesium sulfate tetrahydrate ($MgSO_4 \cdot 4H_2O$, JCPDS no. 00-024-0720). As is shown in Fig. 1(b) and (c), wet magnesia FGD residue consists of irregular particles and its size is about 1–30 μm, the chemical element composition of the wet magnesia FGD residue contained oxygen, magnesium, sulfur and a trace of silicon, calcium, ferric iron. The main mineral phases of the wet magnesia flue gas desulfurization residue were $MgSO_3 \cdot 3H_2O$ and $MgCO_3$ with minor amounts of $MgSO_4 \cdot 7H_2O$ and $MgSO_4 \cdot 4H_2O$.

Vanadium containing industrial wastewater

The wastewater discharged from the sodium roasting vanadium extraction plant was provided by Jianlong Steel Co., Ltd. The concentrations of the main pollutants in the wastewater were as follows: Cr(VI) was 3800 mg L^{-1}, total Cr was 4320 mg L^{-1}, V was 75 mg L^{-1}, NH_4–N was 3200 mg L^{-1} and the pH = 2.14.

Chemical reagents

Potassium dichromate ($K_2Cr_2O_7$), ammonium metavanadate (NH_4VO_3), ammonium chloride (NH_4Cl), sulfuric acid (H_2SO_4), diphenylcarbazide ($C_{13}H_{14}N_4O$), magnesium chloride ($MgCl_2$), sodium hydroxide (NaOH), sodium phosphate (Na_3PO_4), acetone (CH_3COCH_3), Nessler's reagent and sodium potassium tartrate tetrahydrate ($KNaC_4H_4O_6 \cdot 4H_2O$) were purchased from Tianjin Kemiou Chemical Reagent Co., Ltd.

Analysis and detection methods

The acidity was determined using pH detectors (PHS-3E). The 1,5-diphenylcarbazide spectrophotometric method was used to determine the Cr(VI) concentration. The Nessler's reagent spectrophotometry method was used to determine the NH_4–N concentration. Inductively-coupled plasma-optical emission spectrometry (ICP-OES, Optima 8300DV, PerkinElmer) was used to determine the content of total Cr ions, V ions, phosphorus ions and magnesium ions.

The XRD (PW3040/60, Philips) with Cu Kα radiation (λ = 1.54056 Å) was used to identify the crystalline structure of the wet magnesia FGD residue and the coprecipitate at the sweep rate of 6° min^{-1} in the range from 5° to 90°. The scanning electron microscopy-energy dispersive X-ray spectrometry (SEM-EDS, Sigma 500, Zeiss) was used to study the morphology and

Open Access Article. Published on 13 November 2018. Downloaded on 1/16/2025 7:43:59 AM.
This article is licensed under a Creative Commons Attribution-NonCommercial 3.0 Unported Licence.

elemental composition of the wet magnesia FGD residue and the coprecipitate.

Experimental procedure

Batch experiments were performed in a 250 mL glass beaker on a magnetic heated stirrer at room temperature. The diluted NaOH solution and diluted H_2SO_4 solution were used to control the acidity of the reaction solutions during the course of the experiment. Firstly, a certain amount of wet magnesia flue gas desulfurization residue was added into 200 mL of wastewater in a glass beaker with continuous stirring, and the pH of wastewater was controlled at an acidic level until the reduction reaction was completed. Subsequently, a given amount of soluble magnesium and phosphate was added separately into the wastewater to give the desired molar ratio of Mg^{2+}, NH_4^+ and PO_4^{3-} with constant stirring, and the pH of the wastewater was then adjusted to an alkaline level. Finally, the vanadium, chromium and ammonium in the vanadium containing industrial wastewater were removed synchronously by forming the difficult to obtain soluble coprecipitate, and the coprecipitate was then dried at 60 °C before further analysis.

Results and discussion

The main mechanism of the pollutant removal process

In the conventional sodium salt (Na_2CO_3 or NaCl) roasting technique, both vanadium and chromium in vanadium bearing slag were oxidized to a high valence state and then transformed into the soluble vanadate and chromate. The roasted products were washed repeatedly in hot water, and the vanadium raw material was obtained from the high concentration vanadium extraction solution using ammonium polyorthovanadate precipitation in acid conditions.[7,21–25] Therefore, the main existing valences of vanadium and chromium in the wastewater were Cr(VI) and pentavalent vanadium [V(V)], respectively. As is already known, the existing forms of Cr(VI) and V(V) are closely related to their concentration and pH of a solution. Therefore, the existing forms of the Cr(VI) and V(V) were calculated and determined using the Visual MINTEQ aqueous chemical equilibria software based on the actual heavy metal pollutant's concentration in the wastewater. The speciation distribution of Cr(VI) and V(V) were calculated over the range of pH = 0–14.0, as shown in Fig. 2. Consequently, it was found that the main existing forms of heavy metal pollutants in vanadium containing industrial wastewater were $Cr_2O_7^{2-}$ and VO_2^+.[26–28]

The Eh–pH diagrams of Cr–V–S–Mg–H_2O are shown in Fig. 3. Depending on the acidity of the vanadium extraction wastewater (pH = 2.14), the redox potentials of VO_2^+ and $Cr_2O_7^{2-}$ were higher than that of HSO_3^-.[5,7,26–31] Consequently, the VO_2^+ and $Cr_2O_7^{2-}$ could be reduced to VO_2^+ and Cr^{3+} by HSO_3^- which is the acidolysis product of wet magnesia FGD residual (main composition is $MgSO_3 \cdot 3H_2O$), as shown in eqn (1)–(3). In addition, the appropriate low pH condition was conducive to oxidation–reduction reactions because the H^+ also took part in the reaction. At the same time, a large quantity of Mg^{2+} was obtained by the dissolution of $MgSO_3 \cdot 3H_2O$, $MgCO_3$ [as shown in eqn (1) and (4)] and $MgSO_4 \cdot nH_2O$ in the acidic conditions which would be regarded as the low cost magnesium ion source of struvite ($MgNH_4PO_4 \cdot 6H_2O$) crystallization.[32–35] Following the completion of the reductive reaction, the given amount of soluble magnesium and phosphate were added separately into the wastewater. Then, the pH of the wastewater was adjusted to alkalinity. Because the VO^{2+}, Cr^{3+} and NH_4^+ could be separated synchronously from the wastewater by forming an insoluble

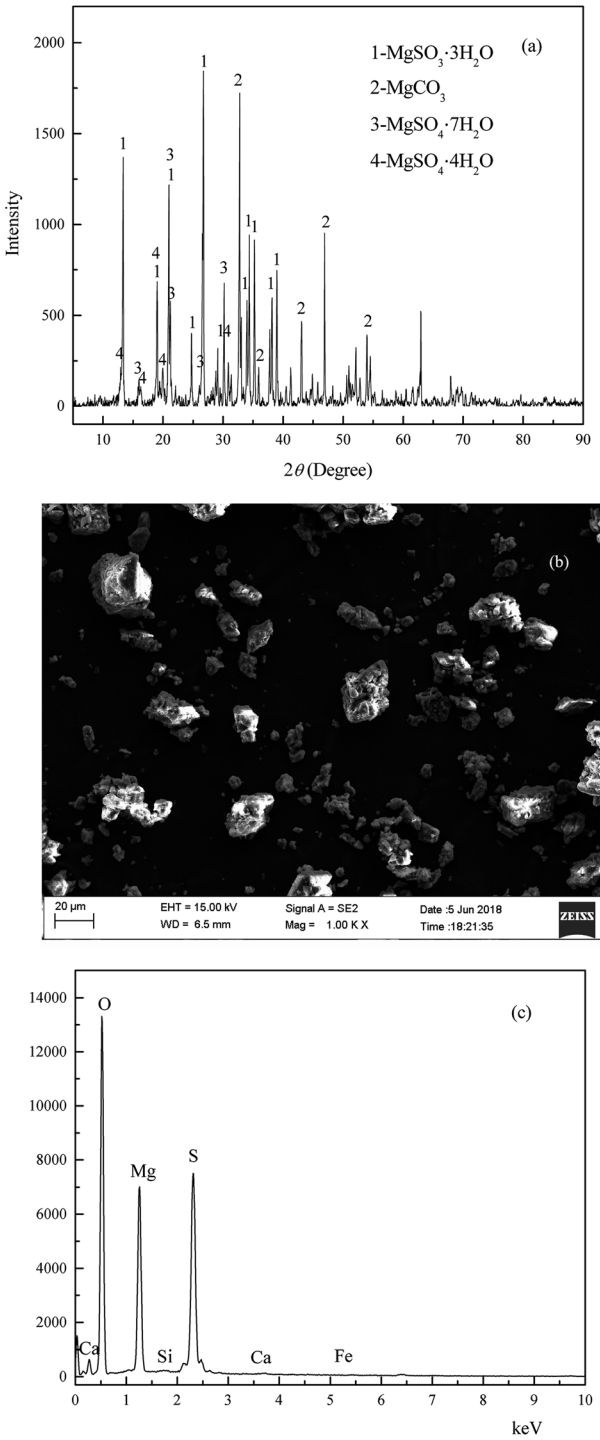

Fig. 1 The XRD (a) and SEM (b) EDS (c) of wet magnesia flue gas desulfurization residue.

Open Access Article. Published on 13 November 2018. Downloaded on 1/16/2025 7:43:59 AM.
This article is licensed under a Creative Commons Attribution-NonCommercial 3.0 Unported Licence.

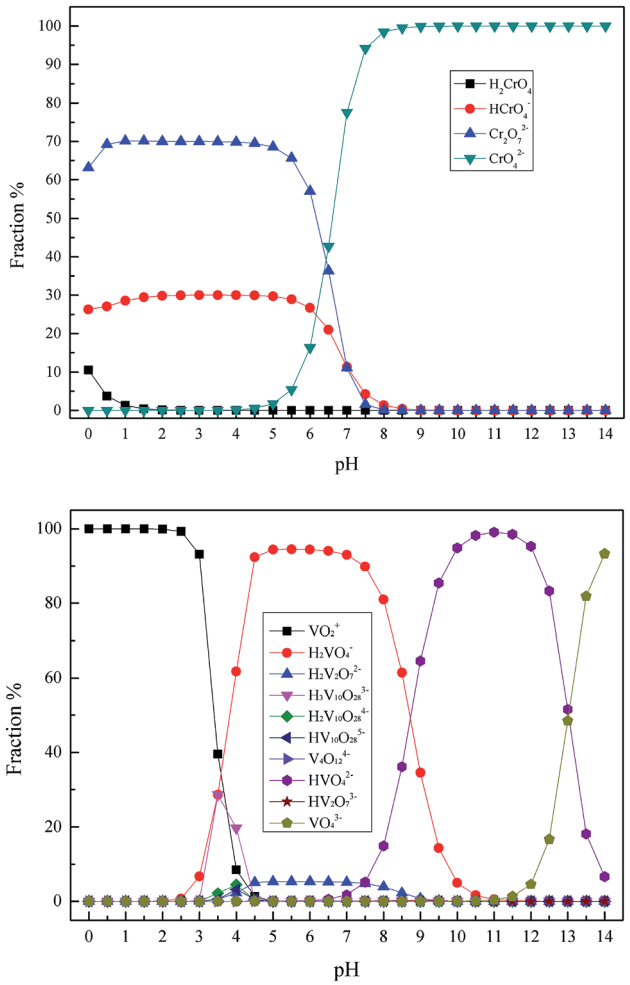

Fig. 2 The species distribution of Cr(VI) and V(V) in aqueous solutions.

sediment including vanadium and chromium hydroxides and struvite in alkaline conditions, as shown in eqn (5)–(7). In conclusion, the simultaneous removal of NH_4–N and heavy metal pollution from vanadium containing industrial wastewater could be realized using wet magnesia FGD residue.

$$MgSO_3\cdot 3H_2O + H^+ \rightarrow Mg^{2+} + HSO_4^- + 3H_2O \quad (1)$$

$$2VO_2^+ + HSO_3^- + H^+ \rightarrow 2VO^{2+} + SO_4^{2-} + H_2O \quad (2)$$

$$Cr_2O_7^{2-} + 3HSO_3^- + 5H^+ \rightarrow 2Cr^{3+} + 3SO_4^{2-} + 4H_2O \quad (3)$$

$$MgCO_3 + 2H^+ \rightarrow Mg^{2+} + CO_2\uparrow + H_2O \quad (4)$$

$$Cr^{3+} + 3OH^- \rightarrow Cr(OH)_3\downarrow \quad (5)$$

$$VO^{2+} + 2OH^- \rightarrow VO(OH)_2\downarrow \quad (6)$$

$$Mg^{2+} + NH_4^+ + HPO_4^{2-} + 6H_2O \rightarrow MgNH_4PO_4\cdot 6H_2O\downarrow + H^+ \quad (7)$$

The optimum pH of the Cr(VI) and V(V) reduction

According to the reductive mechanism of Cr(VI) and V(V), the reductive reaction pH is an important factor to ensure that the Cr(VI) and V(V) could be reduced adequately and rapidly. This experiment was used to determine the optimum pH within the range from 1.5 to 4.5, and the wet magnesia FGD residue dosage was 8.5 g, and reaction time was 15 min.

As shown in Fig. 4, the degree of reduction of Cr(VI) and V(V) is closely related to the pH. Together with an increase of pH from 1.5 to 4.5, the reduction efficiencies of Cr(VI) and V(V) reduced from 99.99% and 99.95% to 98.74% and 99.36%, respectively, and the residual Cr(VI) and V(V) increased from 0.041 mg L^{-1} and 0.035 mg L^{-1} to 47.56 mg L^{-1} and 0.478 mg L^{-1}, respectively. It is worth noting that the main reduction product of Cr(VI) was Cr^{3+} in the pH range from 2.5 to 4.0, as shown in eqn (3). Whereas the main reduction products of Cr(VI) were $Cr(OH)_2^+$ or $Cr(OH)_3$ in the pH range from 4.0 to 4.5, as shown in eqn (8) and (9). The reaction rate of eqn (8) and (9) was slower than that of eqn (3) which resulted in the significant reduction of Cr(VI) reduction efficiency. In the other words, the low pH condition was conducive to the reduction of Cr(VI) and V(V) using wet magnesia FGD residue as a reductant. As required by national Standards, the hazardous heavy metal

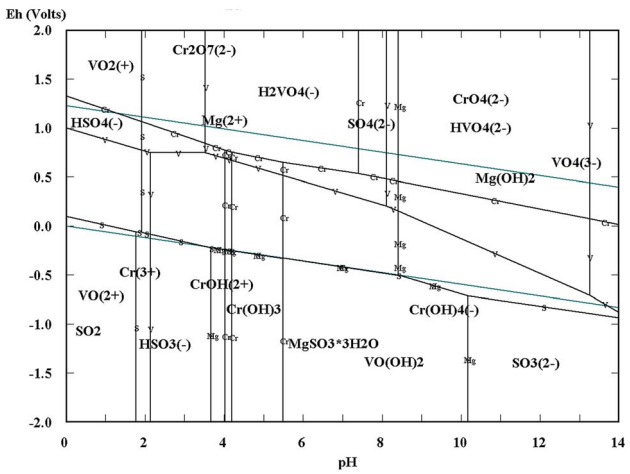

Fig. 3 The Eh–pH diagrams of the Cr–V–S–Mg–H_2O system.

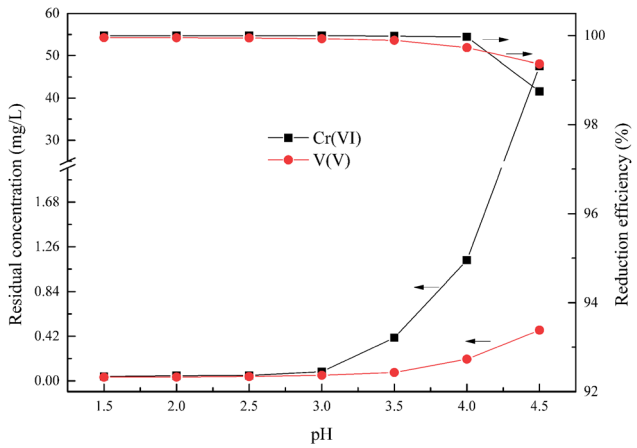

Fig. 4 Effect of pH on Cr(VI) and V(V) reduction. The wet magnesia FGD residue dosage was 8.5 g, and t = 15.0 min.

Open Access Article. Published on 13 November 2018. Downloaded on 1/16/2025 7:43:59 AM.
This article is licensed under a Creative Commons Attribution-NonCommercial 3.0 Unported Licence.

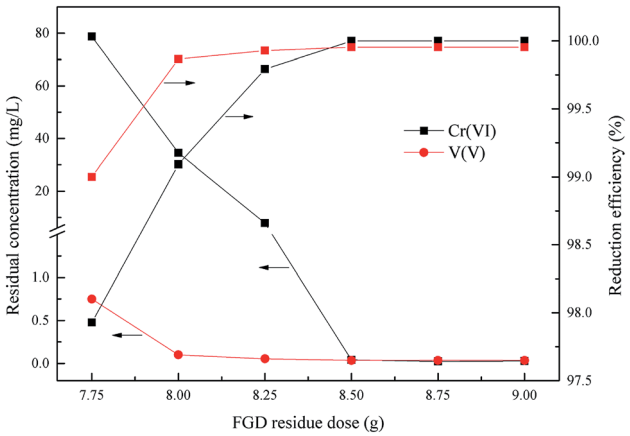

Fig. 5 Effect of wet magnesia FGD dose on Cr(VI) and V(V) reduction. The optimum pH = 2.5, and t = 15.0 min.

pollutants' emission concentration limits of hexavalent chromium and total vanadium were 0.5 mg L^{-1} and 1.0 mg L^{-1}, respectively. In conclusion, the optimum pH of the Cr(VI) and V(V) reduction process was pH = 2.5.

$$Cr_2O_7^{2-} + 3MgSO_3\cdot 3H_2O + 6H \rightarrow 2Cr(OH)_2^{+} + 3SO_4^{2-} + 3Mg^{2+} + 11H_2O \quad (8)$$

$$Cr_2O_7^{2-} + 3MgSO_3\cdot 3H_2O + 2H^{+} \rightarrow 2Cr(OH)_3 + 3SO_4^{2-} + 3Mg^{2+} + 7H_2O \quad (9)$$

The optimum wet magnesia FGD residue dose for Cr(VI) and V(V) reduction

As is already known, the dose of the reducing agent is a key factor of the redox reaction between Cr(VI), V(V) and the wet magnesia FGD residue. This experiment was done to determine the wet magnesia FGD residue dosage within the range from 7.75 g to 9.0 g in 200 mL of wastewater, the optimum reduction pH was 2.5, and the reduction reaction time was 15 min.

As shown in Fig. 5, the degree of reduction of Cr(VI) and V(V) was closely related to the dose of wet magnesia FGD residue. With an increase of the wet magnesia FGD residue dose from 7.75 g to 9.0 g, the reduction efficiency of Cr(VI) and V(V) also increased from 97.92% and 99.0% to 99.99% and 99.95%, respectively, and the residual Cr(VI) and V(V) reduced from 78.7 mg L^{-1} and 0.75 mg L^{-1} to 0.029 mg L^{-1} and 0.035 mg L^{-1}, respectively. Once the dose of wet magnesia FGD residue reached 8.5 g, the reduction efficiency of Cr(VI) and V(V) was steady and the residual pollutant concentration was far below the emission concentration limits. Consequently, the optimum wet magnesia FGD residue dose for Cr(VI) and V(V) reduction was 8.5 g (42.5 g L^{-1}).

The optimum time for Cr(VI) and V(V) reduction

This experiment was carried out to determine the optimum time of Cr(VI) and V(V) reduction within the range of reaction time from 5.0 min to 30.0 min, the optimum reduction pH = 2.5, the optimum wet magnesia FGD residue dose was 8.5 g in 200 mL of wastewater.

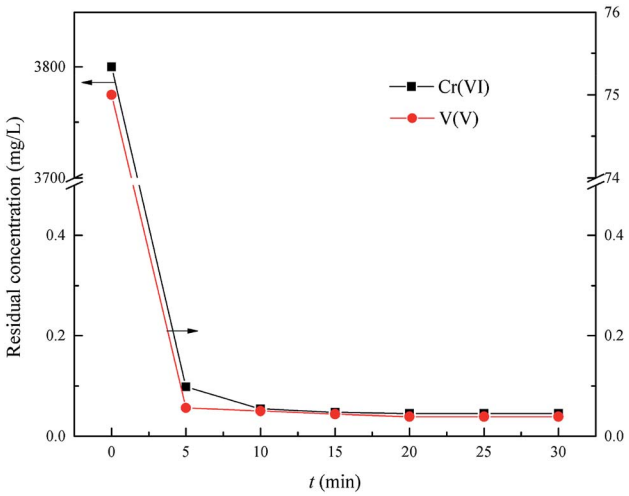

Fig. 6 Effect of reaction time on Cr(VI) and V(V) reduction. The optimum pH is 2.5, and the wet magnesia FGD residue dose is 8.5 g.

As shown in Fig. 6, the residual Cr(VI) and V(V) reduced significantly from the initial 3800 mg L^{-1} and 75 mg L^{-1} to 0.045 mg L^{-1} and 0.039 mg L^{-1}, respectively, with an increase of reduction time from 0 min to 30.0 min, respectively. Therefore, the Cr(VI) and V(V) could be reduced quickly to Cr(III) and V(IV) by using the wet magnesia FGD residue as a reductant within 15.0 min. So, the wet magnesia FGD residue could be regarded as a low cost and environmentally effective substitute for conventional reductants, such as sodium metabisulfite ($Na_2S_2O_5$) or iron(II) sulfate ($FeSO_4$). Consequently, the optimum reduction time was 15.0 min, and the concentration of the by-product, magnesium ions was about 5517 mg L^{-1}.

The optimum pH for ammonium nitrogen and heavy metal pollutants removal

The pH was a key factor for struvite crystallization and the formation of chromium and vanadium hydroxides. This experiment was performed to determine the optimum pH of total chromium, vanadium and ammonium removal within the

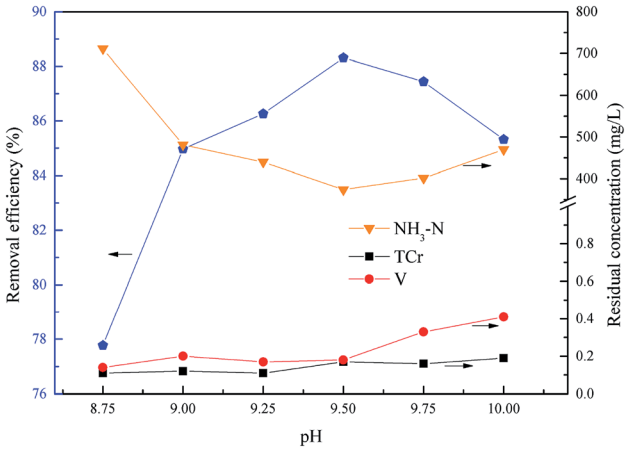

Fig. 7 Effect of pH on NH_4–N and heavy metal pollutants removal. The molar ratio $n(Mg^{2+}) : n(NH_4^{+}) : n(PO_4^{3-})$ = 0 : 1.0 : 1.0, and t = 15.0 min.

Open Access Article. Published on 13 November 2018. Downloaded on 1/16/2025 7:43:59 AM.
This article is licensed under a Creative Commons Attribution-NonCommercial 3.0 Unported Licence.

pH range 8.75 to 10.0, with the molar ratio of $n(Mg^{2+}) : n(NH_4^+) : n(PO_4^{3-}) = 1.0 : 1.0 : 1.0$, and the reaction time was 15.0 min. The molar ratio of the residual Mg^{2+} (5517 mg L^{-1}) and NH_4^+ was about 1.0 : 1.0, so the actual added molar ratio of $n(Mg^{2+}) : n(NH_4^+) : n(PO_4^{3-})$ was 0 : 1.0 : 1.0.

As shown in Fig. 7, the removal efficiency of ammonium increased first from 77.77% to 88.31% and then reduced to 85.32% with an increase of pH, and the ammonium removal efficiency reached a peak at pH = 9.5, and the residual concentrations of chromium and vanadium were always below the emission concentration limits. The main form of phosphate was HPO_4^{2-} in alkaline conditions within the experimental pH range. As shown in eqn (7), the excess H^+ would inhibit the formation of struvite. With the pH increasing, more PO_4^{3-} was dissociated from HPO_4^{2-} which lead to the struvite being replaced by magnesium phosphate [$Mg_3(PO_4)_2$].[34–36] Consequently, the optimum pH of total chromium, vanadium and ammonium removal was 9.5.

The optimum molar ratio of $n(Mg^{2+}) : n(NH_4^+) : n(PO_4^{3-})$ for NH_4–N removal

This experiment was used to determine the optimum molar ratio $n(Mg^{2+}) : n(NH_4^+) : n(PO_4^{3-})$ for NH_4–N removal within 15.0 min. Firstly, the optimum molar ratio between NH_4^+ and PO_4^{3-} was investigated within the range of $n(Mg^{2+}) : n(NH_4^+) : n(PO_4^{3-}) = 0 : 1.0 : 0.9$ to $0 : 1.0 : 1.4$, and the optimum pH = 9.5. As shown in Fig. 8(a), the removal rate of NH_4–N increased first from 83.99% to 89.05% and then reduced slightly to 87.10% together with an increase of the molar ratio $n(Mg^{2+}) : n(NH_4^+) : n(PO_4^{3-})$ from $0 : 1.0 : 0.9$ to $0 : 1.0 : 1.4$. Consequently, the optimum molar ratio between NH_4^+ and PO_4^{3-} was 1.0 : 1.0 because the excess PO_4^{3-} lead to a phosphorus residue with only a little increase of NH_4–N removal.

Subsequently, the optimum molar ratio between Mg^{2+} and NH_4^+ was investigated within the range of $n(Mg^{2+}) : n(NH_4^+) : n(PO_4^{3-}) = 0 : 1.0 : 1.0$–$0.5 : 1.0 : 1.0$, and the optimum pH = 9.5. As shown in Fig. 8(b), with an increase of molar ratio of $n(Mg^{2+}) : n(NH_4^+) : n(PO_4^{3-})$ from 0 : 1.0 : 1.0 to 0.5 : 1.0 : 1.0, the NH_4–N removal rate increased first from 88.46% to 94.25% and then reduced slightly to 94.06%, and the residual phosphorus was also reduced markedly from 540 mg L^{-1} to 12.0 mg L^{-1}. Consequently, the optimum molar ratio of $n(Mg^{2+}) : n(NH_4^+)$ was 0.3 : 1.0.

It is worth noting that the serious overdosing of Mg^{2+} or HPO_4^{2-} would reduce the ammonium removal efficiency, because the concentration of PO_4^{3-} would be increased together with the HPO_4^{2-} increasing because of the dissociation of HPO_4^{2-}, as shown in eqn (10). So, excessive PO_4^{3-} could be consumed before more Mg^{2+} to produce $Mg_3(PO_4)_2$ which would result in a shortage of Mg^{2+} to form struvite, as shown in eqn (11). Also, excessive Mg^{2+} would also consume more PO_4^{3-} to produce $Mg_3(PO_4)_2$ which would result in the shortage of HPO_4^{2-} to form struvite.[7,33,34] Consequently, the optimum molar ratio of $n(Mg^{2+}) : n(NH_4^+) : n(PO_4^{3-}) = 0.3 : 1.0 : 1.0$.

$$HPO_4^{2-} \rightarrow H^+ + PO_4^{3-} \quad (10)$$

$$Mg^{2+} + PO_4^{3-} \rightarrow Mg_3(PO_4)_2 \quad (11)$$

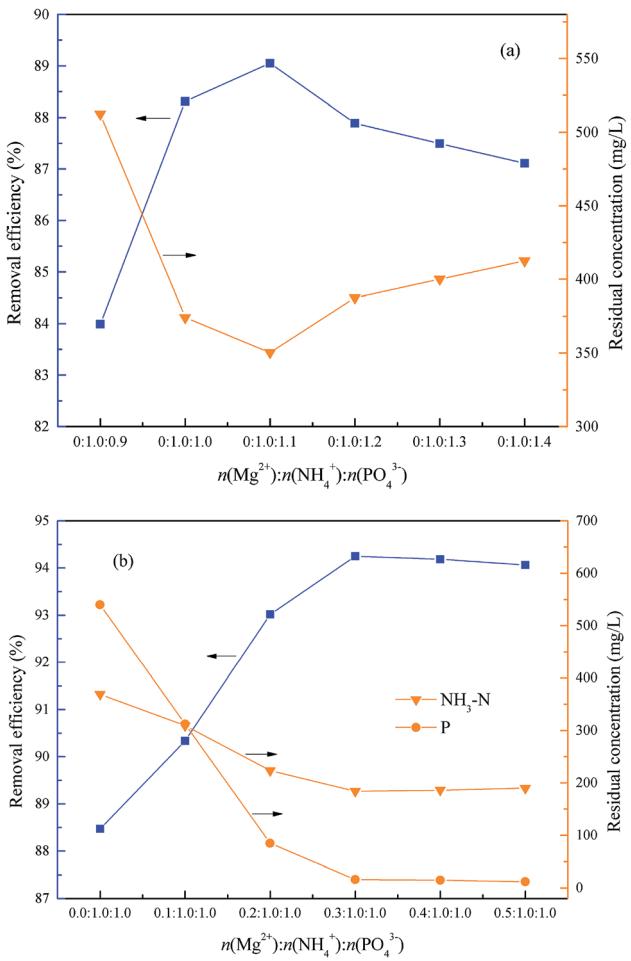

Fig. 8 Effect of the molar ratio $n(Mg^{2+}) : n(NH_4^+) : n(PO_4^{3-})$ on NH_4–N removal. The optimum pH = 9.5 and t = 15 min.

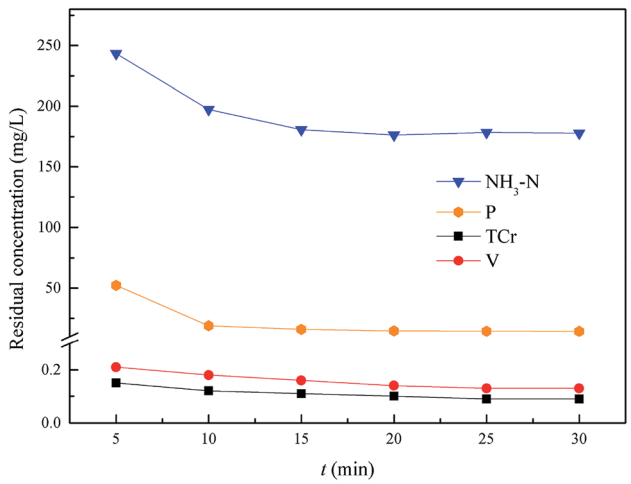

Fig. 9 Effect of NH_4–N and heavy metal pollutant removal. The optimum pH = 9.5, and the molar ratio $n(Mg^{2+}) : n(NH_4^+) : n(PO_4^{3-}) = 0.3 : 1.0 : 1.0$.

Open Access Article. Published on 13 November 2018. Downloaded on 1/16/2025 7:43:59 AM.
This article is licensed under a Creative Commons Attribution-NonCommercial 3.0 Unported Licence.

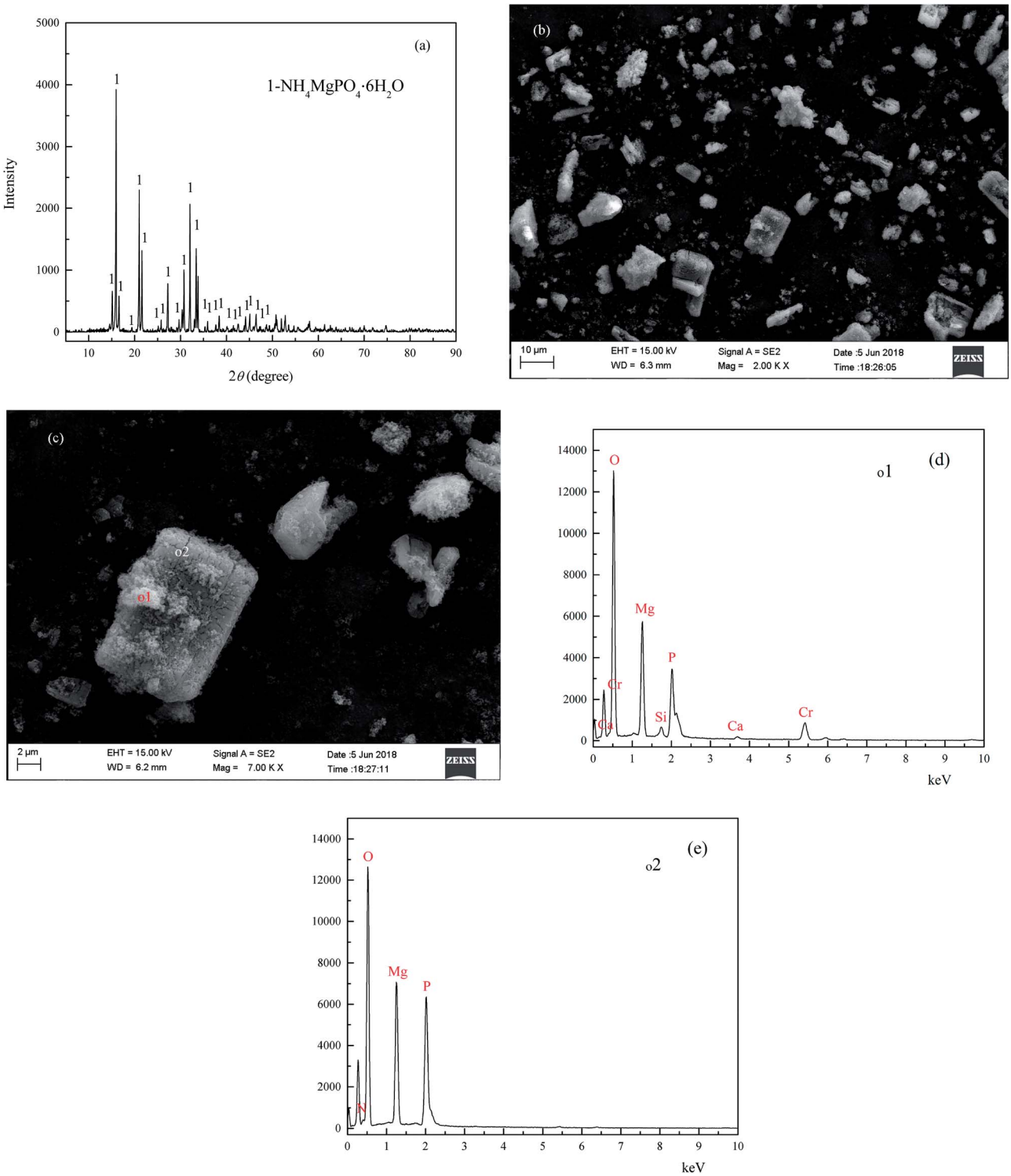

Fig. 10 XRD pattern (a), SEM (b and c) EDS patterns (d and e) of the coprecipitate.

The optimum reaction time for NH_4–N and heavy metal pollutant removal

This experiment was used to determine the optimum reaction time of NH_4–N and heavy metal pollutants from 5.0 min to 30.0 min, with an optimum pH = 9.5, and the optimum molar ratio $n(Mg^{2+}) : n(NH_4^{+}) : n(PO_4^{3-}) = 0.3 : 1.0 : 1.0$. As shown in Fig. 9, the residual NH_4–N and heavy metal pollutants could reach an optimal state and remain stable within 20.0 min. So, the optimum reaction time of NH_4–N and heavy metal pollutants removal was 20.0 min, and the residual pollutant levels were: Cr(VI): 0.047 mg L^{-1}, total Cr: 0.1 mg L^{-1}, V: 0.14 mg L^{-1}, NH_4–N:

Open Access Article. Published on 13 November 2018. Downloaded on 1/16/2025 7:43:59 AM.
This article is licensed under a Creative Commons Attribution-NonCommercial 3.0 Unported Licence.

176.2 mg L^{-1} (removal efficiency was 94.5%) and phosphorus: 14.7 mg L^{-1}.

Characterization analysis of the coprecipitate

The XRD analysis results of the coprecipitate are shown in Fig. 10(a), and the main peaks of the coprecipitate are entirely consistent with $MgNH_4PO_4 \cdot 6H_2O$ (struvite JCPDS no. 01-077-2303). The micrographs of the coprecipitate are shown in Fig. 10(b) and (c), and show some irregular agglomerated particles attached to the surface of the bulk shape crystal. The EDS patterns of the coprecipitate are shown in Fig. 10(d) and (e), and the main chemical element constituent of the bulk shape crystal [o2, Fig. 10(e)] contained O, Mg, N, P, which is consistent with the element constituents of struvite. In comparison, the chemical element constituent of irregular agglomerated particles [o1, Fig. 10(d)] on the surface of the bulk shape crystal contained O, Mg, P, Cr, Ca and Si. The results of the quantitative analysis of the coprecipitate was (wt%): MgO: 17.45, P: 10.32, chromium(III) oxide (Cr_2O_3): 8.27, N: 4.17, Na: 0.29, S: 0.165, V: 0.14, CaO: 0.47, SiO_2: 1.11, and TFe: 0.24. In conclusion, the heavy metal pollutants and NH_4–N in the vanadium containing industrial wastewater were removed by forming the difficult to obtain, soluble coprecipitate containing struvite and chromium and vanadium hydroxide in alkaline conditions.

Conclusions

In this paper, a novel resource utilization method of the wet magnesia flue gas desulfurization residue for simultaneously removing ammonium nitrogen and heavy metal pollutants from vanadium containing industrial wastewater was proven to be viable and effective. The main mineral phases of the wet magnesia flue gas desulfurization residue were $MgSO_3 \cdot 3H_2O$ and $MgCO_3$ with a minor amount of $MgSO_4 \cdot 7H_2O$ and $MgSO_4 \cdot 4H_2O$. The optimum experimental conditions of hexavalent chromium and pentavalent vanadium reduction were: the reduction pH = 2.5, wet magnesia flue gas desulfurization dose was 42.5 g L^{-1}, and the reduction time was 15.0 min. The optimum experimental conditions of ammonium nitrogen and heavy metal pollutants removal were: the precipitate reaction pH = 9.5, the molar ratio $n(Mg^{2+}) : n(NH_4^+) : n(PO_4^{3-}) = 0.3 : 1.0 : 1.0$, and the reaction time was 20.0 min. The residual pollutant concentrations were: chromium(VI) was 0.047 mg L^{-1}, total chromium was 0.1 mg L^{-1}, vanadium was 0.14 mg L^{-1}, ammonium nitrogen was 176.2 mg L^{-1} (removal efficiency was 94.5%) and phosphorus was 14.7 mg L^{-1}. The main pollutants in the vanadium containing industrial wastewater could be removed by forming the difficult to obtain, soluble coprecipitate containing struvite, chromium and vanadium hydroxide.

In general, this research provided a relatively low cost, efficient and environmental treatment process of the vanadium containing industrial wastewater and wet magnesia FGD residue, which has realized the objective of "waste treated using waste".

Conflicts of interest

There are no conflicts of interest to declare.

Acknowledgements

The authors are grateful for the support from the Natural Science Foundation of China (No. U1502273).

References

1 H. Zhang, B. Zhang and J. Bi, *Energy*, 2015, **80**, 1–9.
2 T. Zhu, Y. Ma, H. Zhang, D. Li and L. Li, *Catal. Today*, 2015, **258**, 70–74.
3 X. Liu, B. Lin and Y. Zhang, *J. Cleaner Prod.*, 2016, **113**, 133–143.
4 F. J. Gutiérrez Ortiz, *Chem. Eng. J.*, 2010, **165**, 426–439.
5 D. Fang, X. Liao, X. Zhang, A. Teng and X. Xue, *J. Hazard. Mater.*, 2017, **342**, 436–445.
6 D. Zheng, H. Lu, X. Sun, X. Liu, W. Han and L. Wang, *Thermochim. Acta*, 2013, **559**, 23–31.
7 D. Fang, X. Zhang, M. Dong and X. Xue, *J. Hazard. Mater.*, 2017, **336**, 8–20.
8 Z. Shen, X. Chen, M. Tong, S. Guo, M. Ni and J. Lu, *Fuel*, 2013, **105**, 578–584.
9 L. Wang, Y. Ma, W. Zhang, Q. Li, Y. Zhao and Z. Zhao, *J. Hazard. Mater.*, 2013, **258–259**, 61–69.
10 R. Guo, W. Pan, X. Zhang, H. Xu and J. Ren, *Fuel*, 2011, **90**, 7–10.
11 R. Valle-Zermeño, J. Formosa, J. Aparicio and J. Chimenos, *Chem. Eng. J.*, 2014, **254**, 63–72.
12 L. Wang, S. Cui, Q. Li, J. Wang and S. Liu, *Appl. Catal., A*, 2016, **511**, 16–22.
13 Q. Li, Y. Yang, L. Wang, P. Xu and Y. Han, *Appl. Catal., B*, 2017, **203**, 851–858.
14 L. Guo, W. Liu, X. Tang, H. Wang, Q. Liu and Y. Zhu, *Chem. Eng. J.*, 2017, **330**, 870–879.
15 L. Yan, X. Lu, Q. Guo, Q. Wang and X. Ji, *Adv. Powder Technol.*, 2014, **25**, 1709–1714.
16 L. Yan, X. Lu, Q. Wang, Y. Kang, J. Xu and Y. Chen, *Therm. Eng.*, 2014, **65**, 487–494.
17 Y. Zhang, S. Bao, T. Liu, T. Chen and J. Huang, *Hydrometallurgy*, 2011, **109**, 116–124.
18 R. R. Moskalyk and A. M. Alfantazi, *Miner. Eng.*, 2003, **16**, 793–805.
19 X. Zhang, F. Liu, X. Xue and T. Jiang, *J. Alloys Compd.*, 2016, **686**, 356–365.
20 M. R. Tavakoli, S. Dornian and D. B. Dreisinger, *Hydrometallurgy*, 2014, **141**, 59–66.
21 H. Li, H. Fang, K. Wang, W. Zhou, Z. Yang, X. Yan, W. Ge, Q. Li and B. Xie, *Hydrometallurgy*, 2015, **156**, 12–135.
22 D. He, Q. Feng, G. Zhang, L. Ou and Y. Lu, *Miner. Eng.*, 2007, **20**, 1184–1186.
23 K. Yang, X. Zhang, X. Tian, Y. Yang and Y. Chen, *Hydrometallurgy*, 2010, **103**, 7–11.
24 X. Li, B. Xie, G. Wang and X. Li, *Trans. Nonferrous Met. Soc. China*, 2011, **21**, 1860–1867.

 This journal is © The Royal Society of Chemistry 2018

Open Access Article. Published on 13 November 2018. Downloaded on 1/16/2025 7:43:59 AM.
This article is licensed under a Creative Commons Attribution-NonCommercial 3.0 Unported Licence.

25 Y. Ji, S. Shen, J. Liu and Y. Xue, *J. Cleaner Prod.*, 2017, **149**, 1068–1078.
26 C. Barreradíaz, V. Lugolugo and B. Bilyeu, *J. Hazard. Mater.*, 2012, **223–224**, 1–12.
27 S. Wilson and J. Weber, *Chem. Geol.*, 1979, **26**, 345–354.
28 B. Wehrli and W. Stumm, *Geochim. Cosmochim. Acta*, 1989, **53**, 69–77.
29 J. A. Dean, *Lange's Handbook of Chemistry*, McGraw-Hill, New York, 1999.
30 S. Xu, S. Pan, Y. Xu, Y. Luo, Y. Zhang and G. Li, *J. Hazard. Mater.*, 2015, **283**, 7–13.
31 Y. Yuan, S. Yang, D. Zhou and F. Wu, *J. Hazard. Mater.*, 2016, **307**, 294–301.
32 D. Zhang, Y. Chen, G. Jilani, W. Wu, W. Liu and Z. Han, *Bioresour. Technol.*, 2012, **116**, 386–395.
33 T. Zhang, L. Ding, H. Ren and X. Xiong, *Water Res.*, 2009, **43**, 5209–5215.
34 T. Zhang, L. Ding and H. Ren, *J. Hazard. Mater.*, 2009, **166**, 911–915.
35 H. Huang, D. Xiao, Q. Zhang and L. Ding, *J. Environ. Manage.*, 2014, **145**, 191–198.
36 S. Zhou and Y. Wu, *Environ. Sci. Pollut. Res. Int.*, 2012, **19**, 347–360.